Communication in Physical Sciences, 2025, 12(8):2280-2299

Synthesis, Characterization and *In-Silico* Study of Mn (II) And Zn (II) Nano-Sized Complexes Of Metronidazole Synthesized via Sonication Method

Etim, Idongesit George *, Brendan Chidozie Asogwa, Ifeanyi Edozie Otuokere, Kelvin O. Amadi

Received:14 September 2025/Accepted: 06 December 2025/Published: 25 December 2025
https://dx.doi.org/10.4314/cps.v12i8.9

Abstract: *This study reports the sonochemical synthesis, physicochemical characterization, and in-silico evaluation of Mn (II) and Zn (II) nano-sized complexes of metronidazole (MTZ), a known oral antibiotic drug. The complexes were synthesized using sonication mechanism and characterized using UV–Vis, FT-IR, XRD, TEM, and NMR techniques. Notable and distinct changes in colour, melting point, solubility, and spectral characteristics confirmed a successful coordination of MTZ to Mn (II) and Zn (II) ions. XRD analysis of the compounds revealed nanocrystalline phases measuring 26–83 nm, while TEM images showed particle sizes within 2.22–10.80 nm, confirming nanoscale formation. NMR spectra indicated the metal coordination through the imidazole nitrogen and, in the case of Mn (II), partial involvement of the hydroxyl oxygen. ADMET and toxicity predictions using SwissADME and ProTox-II showed high gastrointestinal absorption, good solubility, high bioavailability scores, and toxicity class IV for all compounds. These findings support the potential of Mn (II)–MTZ and Zn (II)–MTZ nanocomplexes as promising candidates for drug design and antimicrobial applications.*

Keywords: *Metronidazole, sonochemistry, in silico, Mn (II), Zn (II)*

George Idongesit Etim*
Department of Chemical sciences, Akwa Ibom State Polytechnic, Ikot Osurua, Ikot Ekpene, Akwa Ibom State, Nigeria
Email: idygeorgevision@gmail.com
Orcid id: https://orcid.org/0009-0007-1183-5141

Brendan Chidozie Asogwa
Department of Chemistry, Michael Okpara University of Agriculture, Umudike, Abia State, Nigeria
Email: chidonwasogwa@gmail.com
Orcid id: https://orcid.org/0009-0009-8530-9982

Ifeanyi Edozie Otuokere
Department of Chemistry, College of Physical and Applied Sciences, Michael Okpara University of Agriculture, Abia, Nigeria.
Email: ifeanyiotuokere@gmail.com
Orcid id: https://orcid.org/0000-0003 0038-8132

Kelvin O. Amadi
Department of Chemistry, College of Physical and Applied Sciences, Michael Okpara University of Agriculture, Abia, Nigeria.
Email: amadikelvin77@gmail.com

1.0 Introduction

Metronidazole (MTZ) is a nitroimidazole derivative widely known for its antibiotic and antiprotozoal effects especially in the treatment of anaerobic bacteria and parasitic infections (Lofmark *et al.,* 2010). The clinical use of metronidazole has been met with issues ranging from microbial resistance, side effects and even suboptimal pharmacokinetic properties (Singh *et al.,* 2012). These have gingered the necessity of research into the development of metal-containing drugs especially clinically viable drugs as a mode of enhancing their therapeutic potentials (Otuokere, 2019). The formation of metal complexes of organic drugs with transition

metal ions has emerged as a promising strategy for combating the growth in antibacterial resistance (Asogwa & Otuokere, 2024). Several of the formed metal complexes of known drugs have been identified to exhibit altered physiochemical properties, novel mechanism of actions and enhanced biological properties when compared to their respective ligands (Otuokere *et al.,* 2016). Transition metal coordination has also in addition so the earlier mentioned benefits also increase the drug stability, solubility and bioavailability especially when they are of nano-range sizes (Guo & Sadler, 2000).

The formulation of metallodrugs in nano sizes has in recent times gained a significant attention. This is due to the discovery that nanoscale modification can significantly alter the physicochemical properties and even interaction with targets in biological systems (Otuokere, 2017). Sonochemical synthesis which is one of the green methods of nano formulation generates compounds with highly improved homogeneity, smaller sized particles and even enhanced reactivity (Robert *et al.,* 2025). Nano metal complexes of manganese and zinc have shown a strong viability which is ascribed to the several biological roles played by these metals especially their enzymatic or redox actions which are relevant in disease management (Andreini *et al.,* 2008; Asogwa *et al.,* 2024). The biocompatibility of manganese and zinc makes their use in the synthesis of metal complexes very useful (Singh *et al.,* 2012). The XRD and TEM studies have shown that nano-sized metal complexes of drugs (metallodrugs) usually show very unique morphology and crystallite sizes which contribute to their improved biological relevance (Smith *et al.,* 2020; Lee *et al.,* 2021). The increased use of computational studies tools such as *in-silico* is hinged on its ability to provide a cost-effective and rapid predictions of the pharmacokinetic behavior, drug-likeness, and toxicity properties of novel compounds (Asogwa & Otuokere, 2024; Otuokere *et al.,* 2025). The predicted properties compliment the obtained laboratory characteristics by predicting and estimating the gastrointestinal absorption, bioavailability, water solubility, inhibition of enzyme and even the toxicity class which are important parameters in drug development (Otuokere *et al.,* 2025) and so guides the selection of promising candidates for further experimental studies (Daina *et al.,* 2017). Although these tools have been widely used on several forms of compounds, but their application to nano-sized complexes of metronidazole have not been explored in literature. A review of literature revealed limited available researches on the integration of sonochemical synthesis of nanosized compounds and detailed spectroscopic characterization with *in-silico* (ADMET) predictions. Therefore, this study is aimed at synthesizing and characterizing nanometal complexes of metronidazole and also predicting their pharmacokinetic properties and toxicity profile.

The development of nano-sized Mn(II)–MTZ and Zn(II)–MTZ complexes through sonochemical synthesis presents a promising approach for overcoming the limitations associated with conventional metronidazole therapy, including microbial resistance, low bioavailability, and adverse drug responses. The nanoscale formulation is expected to improve drug solubility, stability, and pharmacokinetic performance, while metal coordination may introduce new mechanisms of antimicrobial action. Furthermore, integrating advanced spectroscopic characterization with in-silico ADMET and toxicity prediction provides an early-stage evaluation of the drug-likeness and safety profiles of the synthesized complexes, reducing experimental cost and time. This study therefore offers a novel pathway for the rational design of metallodrugs based on clinically established antibiotics and lays the groundwork

for future antimicrobial drug development using green sonochemical methods.

2. 0 Materials and Methods

2.1 Chemicals and solvents

Salts and Reagents used for this study were all of analytical grade and used without any purification. The MTZ salt was obtained from Andhra Organics Limited India. $MnCl_2 \cdot 4H_2O$ and $Zn(NO_3)_2 \cdot 6H_2O$ were obtained from Sigma-Aldrich.

2.2 Sonochemical Synthesis of Mn (II) and Zn (II) nanocomplexes

The nanometal complexes were synthesized using an ultrasonic sonicator following the procedure reported by Asogwa *et al.,* (2024). A 0.05 molar solution of MTZ (8.6 g) was added to each of 0.1 mol solution of $MnCl_2.4H_2O$ (9.89 g) and of $Zn(NO_3)_2.6H_2O$) (14.87 g). The resultant mixtures were stirred and positioned in an ultrasonic probe of an ultrasonic sonicator operating at 24 kHz with a maximum force output of 400 W, temperature of 50 °C for 30 minutes. The obtained mixtures were then filtered with a Whatman No 1 filter paper. The filtrates were then carefully kept in the desiccator to dry. Each of the complexes was stored in a neatly labelled container after determining their percentage yield.

The synthesis of the novel metal complexes of Metronidazole is proposed as:

$$\mathbf{MnCl_2 \cdot 4H_2O + 2C_6H_9N_3O_3 \rightarrow [Mn(C_6H_9N_3O_3)_2] + 4H_2O + Cl_2}$$

$$\mathbf{Zn(NO_3)_2 \cdot 6H_2O + 2\ C_6H_9N_3O_3 \rightarrow [Zn(C_6H_9N_3O_3)_2] + 2NO_2 + O_2 + 6\ H_2O}$$

2.3. Physical parameters

Using the Gallenkamp melting point equipment, the melting points (in degrees) of the nanometal complexes were determined. Different polarity solvents, such as n-hexane, ethanol, water, ethyl acetate, and dimethylsulfoxide (DMSO) were used to test the solubility of MTZ and the nanometal complexes.

2.4 Characterization

The UV/visible spectral measurements were obtained using a UV-1800 series using dimethoxysulfoxide as solvent in the 200 – 800 nm range. The FT-IR spectra spectra were obtained using a Perkin Elmer Spectrum BX FT-IR spectrophotometer (4400 - 600 cm^{-1}) in KBr pellets. The NMR spectra measurements were obtained on a Nanalysis X-685 benchtop NMR. The X-ray diffraction patterns were obtained using a Rigaku D/Max-lllC X-ray diffractometer. While the morphology

2.4. In-silico studies

2.4.1. ADMET predictions

The ADMET, drug-likeness and interactions were predicted using the Swiss ADME online tool (http://www.swissadme.ch).

2.4.2. Toxicity

The toxicity prediction was done using the ProTox-II online tool (https://tox.charite.de/protox3/index.php?site=compound input).

3.0 Results and Discussion

The physical properties of the free ligand (metronidazole) and the synthesized Mn(II)–MTZ and Zn(II)–MTZ nanocomplexes were examined to provide preliminary evidence of complex formation. Changes in colour appearance, melting point and percentage yield are among the early indicators of successful metal coordination, as coordination often alters the electron environment of the ligand and increases the thermal stability of the resulting complexes. The results are summarized in Table 1.

As shown in Table 1, metronidazole was obtained as a white crystalline solid with a melting point of 160 °C. Upon complexation with Mn(II), the product exhibited a pastel pink colour and a pronounced increase in melting point to 207 °C, indicating enhanced stability

and the formation of a new coordination compound. Similarly, the Zn(II) complex was isolated as a white solid with a melting point of 203 °C, reflecting a thermal stabilization relative to the parent ligand. The percentage yields of the Mn(II) and Zn(II) complexes were 82% and 78%, respectively, demonstrating the efficiency of the sonochemical synthesis approach. The variation in the melting points and colour relative to the free ligand further supports the successful formation of the corresponding metal complexes.

Table 1: Physical properties of the compounds

Compounds	Colour	MP (°C)	% Yield
MTZ	White	160	-
[Mn(MTZ)]	Pastel pink	207	82
[Zn(MTZ)]	White	203	78

MTZ and its complexes are crystalline, stable and non-hydroscopic compounds. A change in colour from white to pastel pink (Table 1) for the Mn (II) complex showed a coordination occurred with a transition metal ion (Otuokere, *et al.,* 2019). Also, the retention of white color for Zn (II) complex aligns with earlier studies of Zn ion not forming colored compounds as it has filled 3d orbitals. (Trupti *et al.,* 2019). An increase in melting point also supports the formation of complexes (Asogwa *et al.,* 2024). The solubility behaviour of the synthesized nanocomplexes was investigated in solvents of varying polarity to assess changes in physicochemical properties arising from metal coordination. Solubility is a key factor influencing bioavailability, membrane permeability and drug formulation behaviour, and metallation has been reported to alter the solvation characteristics of organic ligands. The solubility profiles of metronidazole and its Mn(II) and Zn(II) nanocomplexes in both polar and non-polar solvents are presented in **Table 2**.

As observed in **Table 2**, the free ligand, metronidazole, exhibited solubility in polar solvents including distilled water, ethanol, ethyl acetate and DMSO, while it was insoluble in n-hexane, indicating its hydrophilic character. Upon coordination with Mn(II) and Zn(II), the resulting nanocomplexes retained a similar solubility pattern, showing solubility in all polar solvents tested and remaining insoluble in n-hexane. This trend suggests that complexation does not negatively affect the inherent solubility profile of metronidazole but may enhance polarity-driven dissolution. The solubility of all complexes in DMSO further confirms their suitability for spectroscopic and biological studies requiring polar organic solvents.

Table 2: The Solubility profile of the test compounds

Compounds	n-hexane	Distilled water	Ethanol	Ethyl Acetate	DMSO
MTZ	IS	SS	S	S	S
[Mn(MTZ)]	IS	S	S	S	S
[Zn(MTZ)]	IS	S	S	S	S

MTZ, Mn (II) and Zn (II) nano complexes were all observed to be insoluble in non-polar n-hexane (Table 2) but soluble in polar organic solvents (ethyl acetate, ethanol and DMSO) which is ascribed to the compounds having polar ends with aromatic rings (Ndahi *et al.,* 2018). The Mn (II) and Zn (II) nanocomplexes were observed to be soluble in water (Table 2) ascribed to an increased polarity of the compound by attachment to a metal (Edozie *et al.,* 2020).

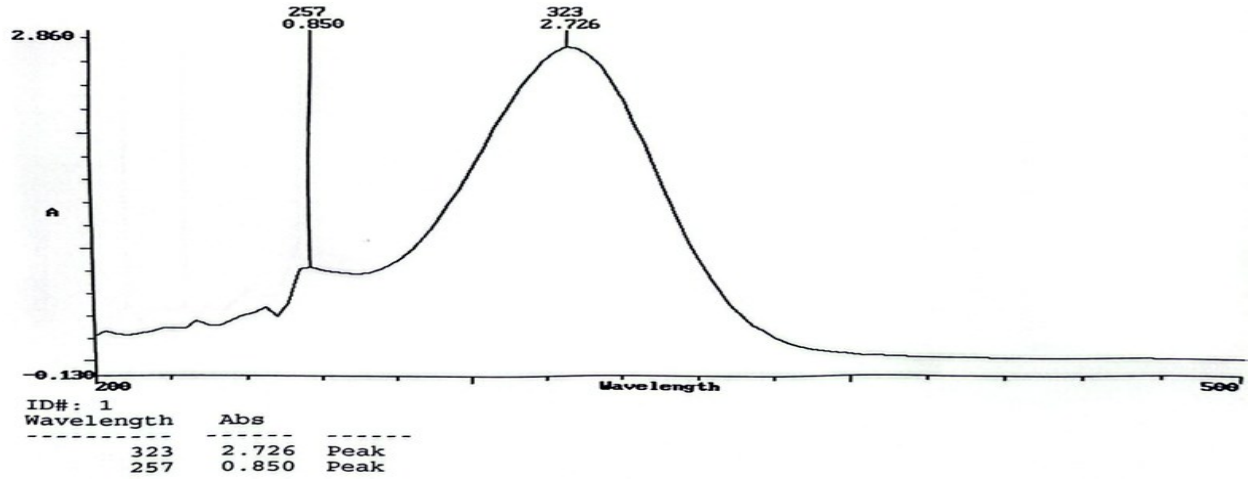

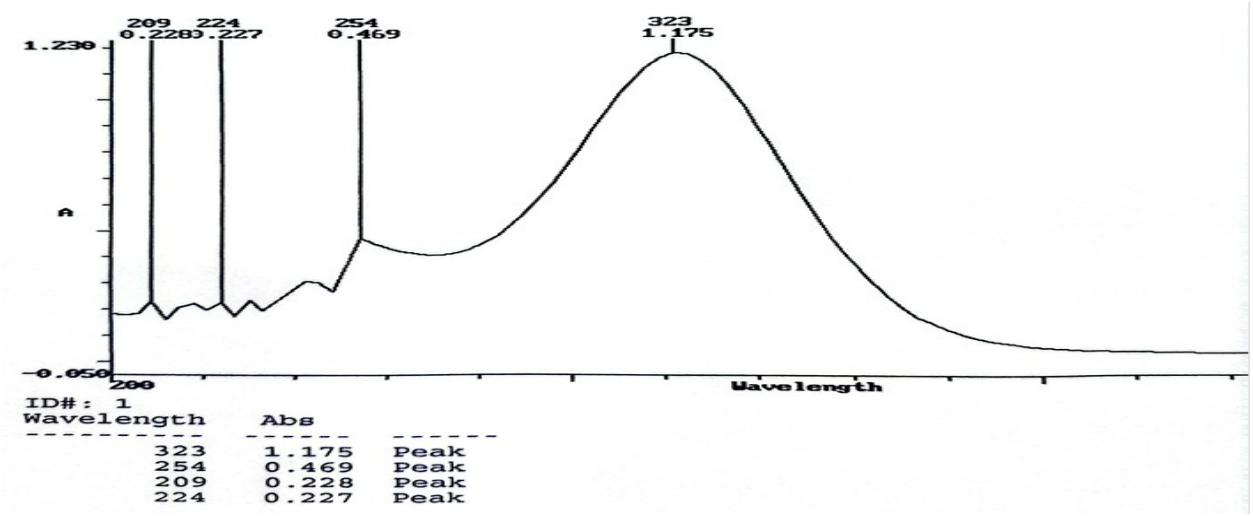

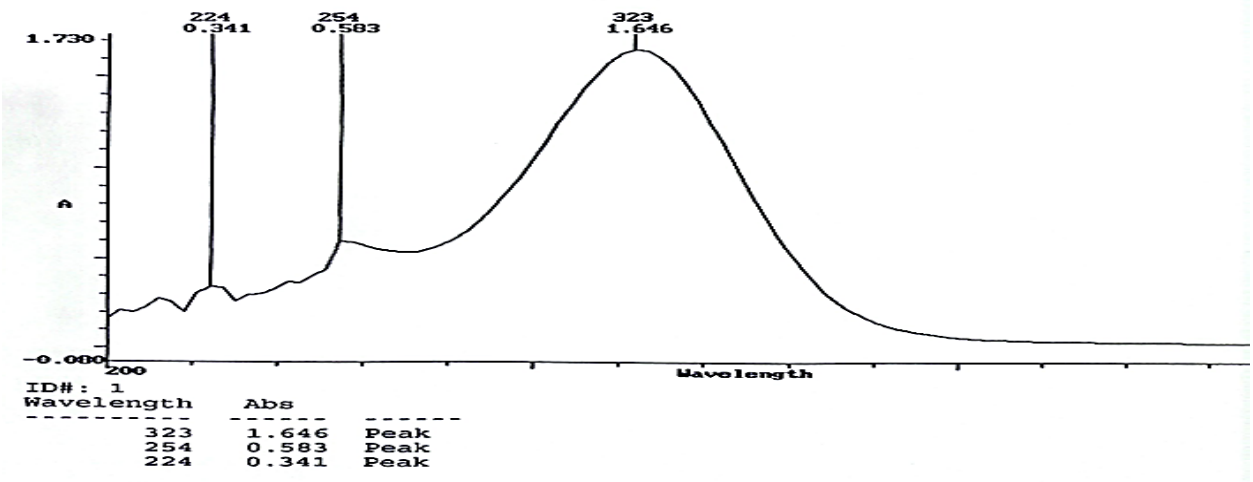

Fig 1: UV/VIS spectrum for MTZ, [Mn(MTZ)], [Zn(MTZ)]

The absorptions observed at λ = 257, 224 and 254 nm in the electronic spectra of MTZ (Fig 1) and its nano complexes was assigned to the π→π* (Onyegbule *et al*., 2021). Also, the

absorptions at λ = 323 nm for all the test compounds were assigned to n→π*. These transitions are due to the compounds containing similar chromophores in their structure (Asogwa & Otuokere, 2024). The Observed peak at λ = 209 and 224 nm for Mn (II) and Zn (II) are assigned to d-d and n→π* transitions respectively (Sadeek *et al*., 2015; Onyegbule *et al*., 2021).

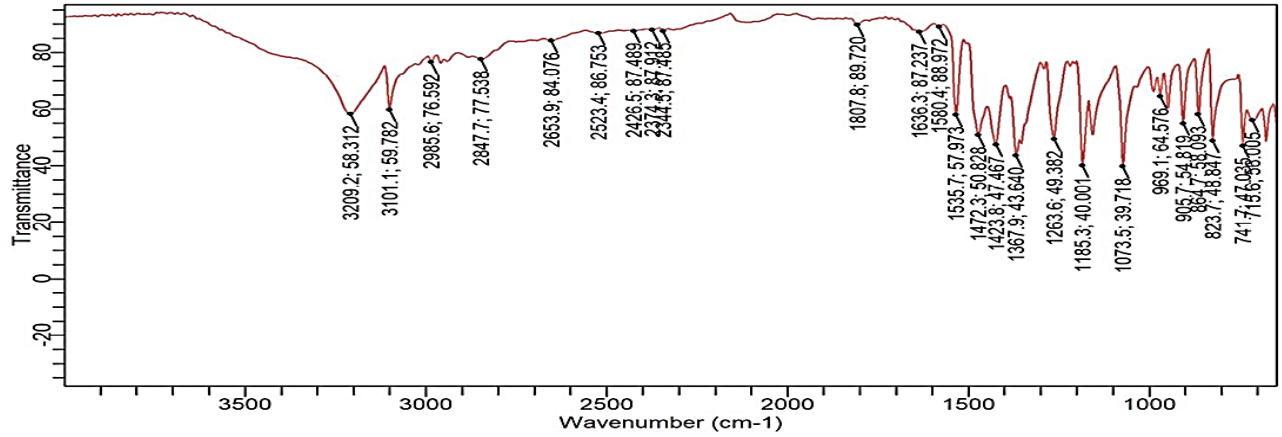

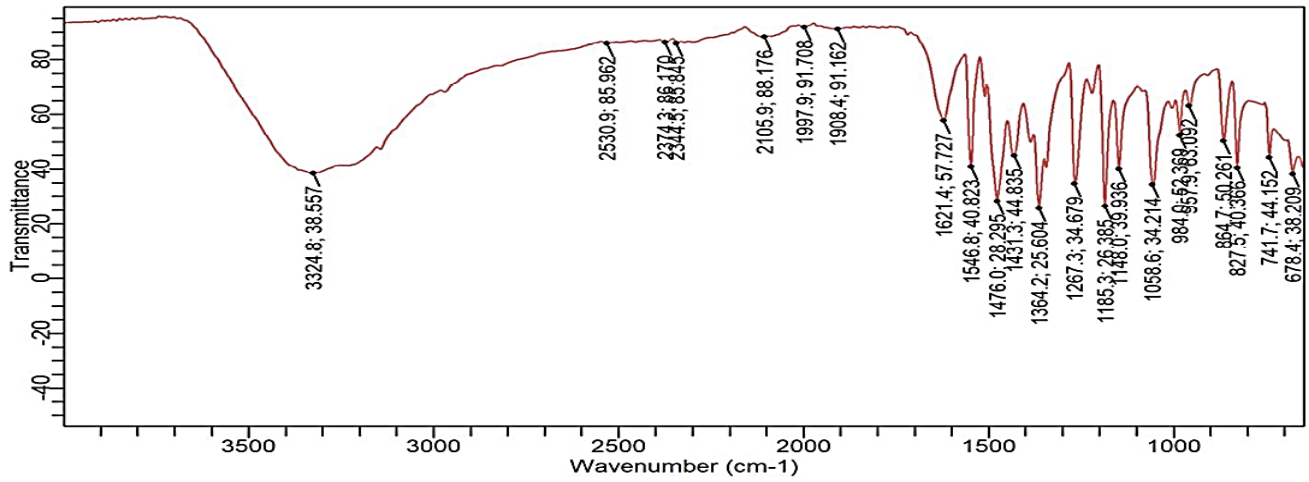

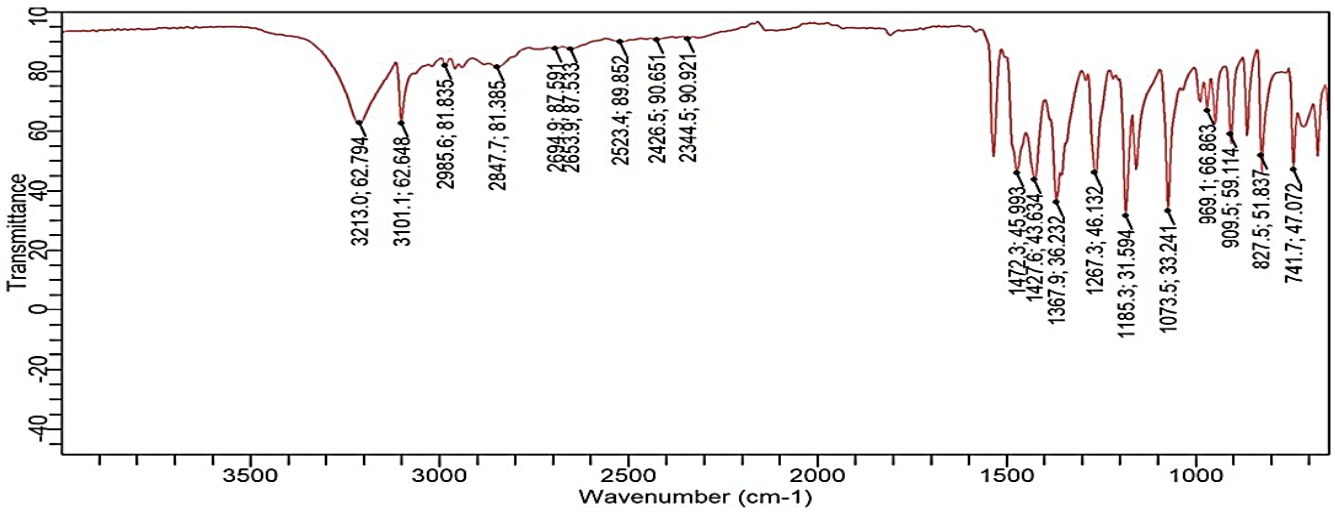

Fig 2: FTIR spectra for MTZ, [Mn(MTZ)], [Zn(MTZ)]

The band at 1636 cm^{-1} assigned to C=N bond of MTZ **(Fig 2)** had a red shift to 1621 and 1550 cm^{-1} for the Mn (II) and Zn (II) nanocomplexes respectively showing coordination to metal ions through the imidazole N1 atom (El-Wahab *et al.,* 2019, Singh *et al.,* 2012). A blue shift was also observed in the band for asymmetric NO_2 observed from 1536 for MTZ to 1546 and 1550 cm^{-1} for Mn (II) and Zn (II) nano complexes respectively indicating coordination through one of the oxygen atoms (El-Wahab *et al.,* 2019). The spectrum of Zn (II) nano complex (Fig 2) showed a significant blue shift (higher wavelength) from 3209 cm^{-1} (of MTZ) to 3325 cm^{-1} corresponding to the OH vibrations. This shift is ascribed to the change in the electron density around the bond when a bond is formed between a metal and oxygen atom of OH (Sadeghi & Azhdari, 2013).

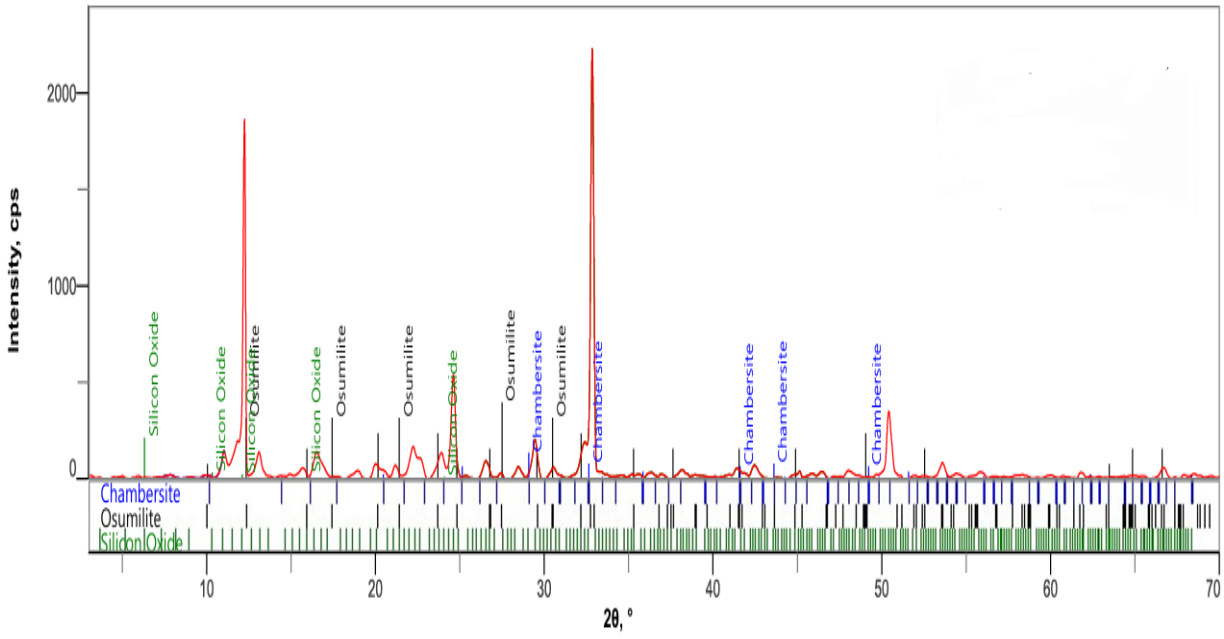

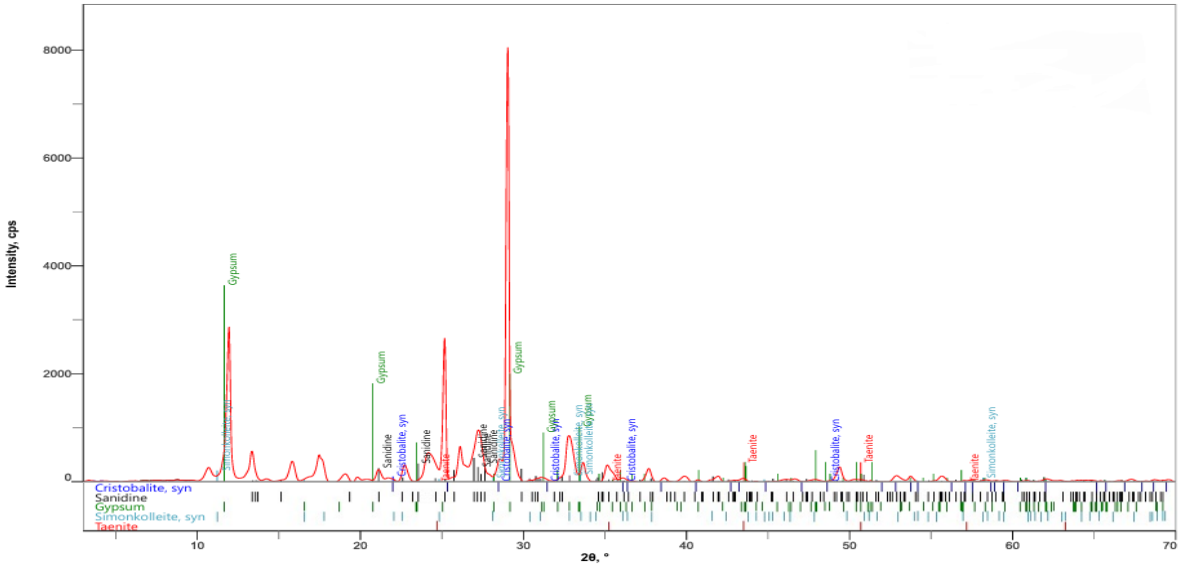

Fig 3: XRD pattern for [Mn(MTZ)], [Zn(MTZ)]

The XRD patterns for the metal complexes confirmed the formation of manganese (Mn) and zinc (Zn) complexes of the ligand metronidazole. This is seen evidently by the dominant crystalline phases containing these metals. For the Mn complexes, the presence of Mn-bearing phases such as Chambersite ($Mn_3B_7O_{13}Cl$) and Braunite ($Mn_7(SiO_4)O_8$) aligns with previous studies showing that Mn (II) readily forms stable complexes with nitrogen and oxygen sites of ligands (Smith *et al*., 2020). The larger crystallite size of 61.6 nm (calculated using Debye Scherrer's equation) suggests high crystallinity for the synthesized complex. This result is consistent with several studies concluding that Mn complexes exhibit strong coordination geometry (Jones & Zhang, 2019). In contrast, the Zn complex displayed phases like Hemimorphite ($Zn_4(Si_2O_7)(OH)_2 \cdot H_2O$) and Simonkolleite ($Zn_5(OH)_8Cl_2 \cdot H_2O$). This agrees with earlier studies that Zn (II) binding usually favors either tetrahedral or octahedral structured coordination with ligands such as metronidazole (Lee *et al*., 2021). The smaller crystallite size of 48.1 nm compared to Mn complex reflects the differences in nucleation kinetics, as Zn complexes often exhibit faster precipitation rates (Brown *et al*., 2018). These findings are consistent with literature reports on metal-drug complexes, where Mn and Zn form distinct crystalline structures depending on ligand interactions (Taylor *et al*., 2022).

Fig. 4 presents the transmission electron microscopy (TEM) micrographs of the synthesized metronidazole metal nanocomplexes, [Mn(MTZ)] and [Zn(MTZ)], recorded at different magnifications to reveal their particle morphology, distribution, and nanoscale structural features. Panels (a–c) correspond to the [Mn(MTZ)] complex, while panels (d–g) show the micrographs of the [Zn(MTZ)] complex. The images highlight the influence of metal coordination on crystal nucleation, growth pattern, particle size uniformity, and agglomeration behaviour. Particle diameters were determined directly from the TEM images, and the measured size distributions are indicated on the micrographs for clarity.

At low magnification (20 nm scale), the [Mn(MTZ)] complex shows diffuse

nanoparticle distribution with regions of dense contrast indicating the presence of aggregated nanocrystallites. The particle boundaries are not sharply defined at this scale, suggesting the early stages of nucleation and particle coalescence. The irregular contrast patterns indicate heterogeneous growth domains consistent with polycrystalline aggregation.

At 50 nm magnification, the nanoparticles appear more clearly resolved, showing a semi-dispersed arrangement. The observed nanostructures exhibit a wide distribution of shapes and densities, with clusters forming in localized regions. This clustering suggests that Mn(II) coordination produces multiple nucleation sites that merge during crystal growth, leading to a less uniform nanostructure. The tendency toward agglomeration at this stage is indicative of lower stabilization efficiency during the nucleation process.

The high-magnification image (100 nm scale) shows particles with defined size ranges from approximately 5.22 to 8.52 nm. The particles display an irregular morphology, with non-spherical shapes dominating the image. This observation confirms the presence of polycrystalline particles, where crystalline domains grow with heterogeneous orientation. The variation in particle geometry and clustering implies that Mn(II) acts as a less controlled nucleation centre, resulting in particles with broader size distribution and agglomerated domains.

The low magnification image (20 nm scale) of [Zn(MTZ)] shows more defined nanoparticle clusters, with distinct spherical particles forming organized aggregates. The clearer contrast between individual particles suggests more mature nanocrystal development. Unlike the Mn complex, Zn-based particles exhibit more cohesive structures where nanocrystals appear to assemble while retaining individual boundaries, indicating controlled crystal growth.

At 50 nm magnification, nanoparticles become distinctly visible with sizes ranging from 2.22 to 3.80 nm at the smallest scale. This strong presence of sub-5 nm particles demonstrates efficient nucleation and slower growth kinetics, a characteristic of Zn(II)-stabilized nanocomplexes. The more monodisperse appearance and spherical morphology indicate superior stabilization of the metronidazole ligand shell around Zn centers, promoting a quantum confinement effect. The emergence of these smaller, well–separated particles suggests that Zn(II) coordination suppresses excessive crystal aggregation.

At higher magnification (100 nm scale), the Zn complex displays a wider size distribution extending from approximately 5.30 to 10.80 nm, with most particles retaining a spherical form. The increase in particle size at this scale reflects secondary growth and cluster formation, where primary nano-sized crystallites assemble into larger superstructures. Despite the broader size range observed at this scale, the particles remain more uniform in shape than the Mn counterpart. This behaviour demonstrates that Zn(II) coordination allows progressive crystal growth while maintaining structural order.

The TEM images clearly demonstrate that metal coordination significantly influences the nucleation and growth mechanism of metronidazole nanocomplexes. The [Mn(MTZ)] complex forms particles predominantly within 5.22–8.52 nm, displaying irregular morphology and pronounced agglomeration. This behaviour is indicative of polycrystalline growth with multiple competing crystal domains initiated by Mn(II), resulting in particles of uneven geometry.

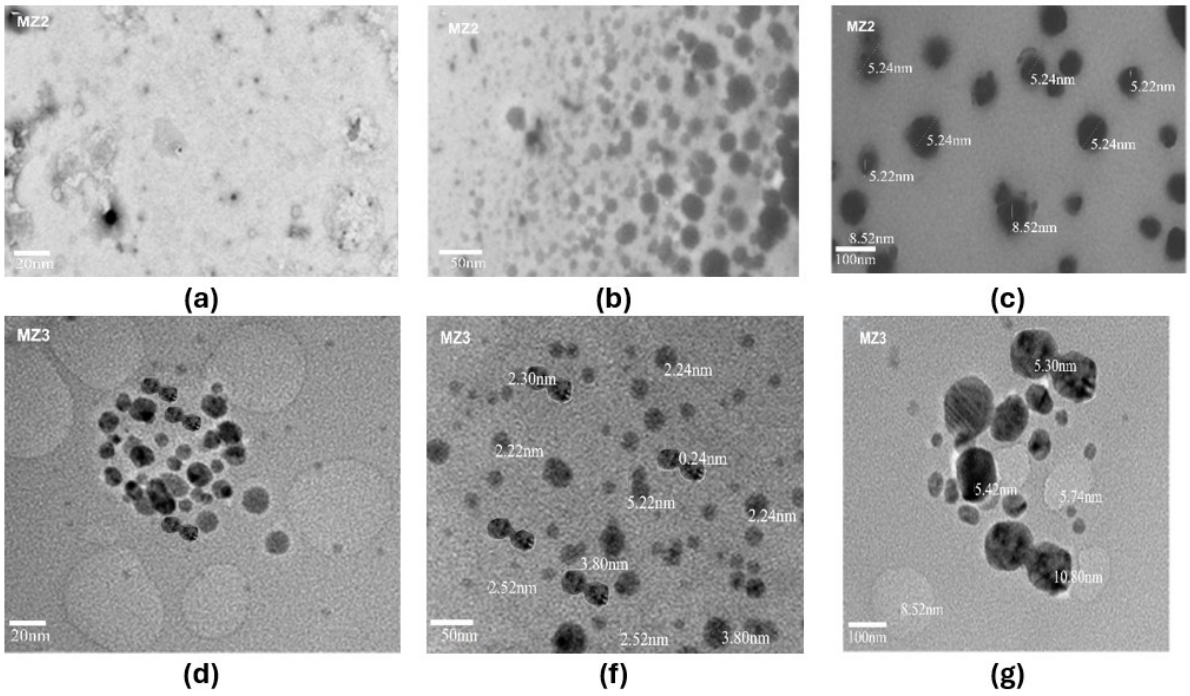

Fig 4: TEM monographs of [Mn(MTZ)] and [Zn(MTZ)]

T In contrast, the [Zn(MTZ)] complex exhibits a broader size distribution (2.22–10.80 nm), although the particles are more uniform and predominantly spherical. The presence of smaller nanoparticles at higher magnification (≈2.22–3.80 nm) highlights early-stage nucleation and suggests a quantum confinement influence driven by Zn(II) coordination. The stabilizing effect of Zn(II) promotes orderly nucleation and retards uncontrolled crystal coalescence, leading to well–defined nanostructures. This trend aligns with earlier reports, where Zn complexes typically produce finer and more defined nanoparticles than Mn analogues due to their superior coordination stability and ligand field characteristics (Lee *et al*., 2021).

The improved homogeneity and smaller-sized domains observed for the Zn complex may have practical implications in drug delivery, where size uniformity enhances cellular uptake and bioavailability. Smaller, well–dispersed nanoparticles can exhibit enhanced antimicrobial activity and sustained release behaviour, as reported for Zn-based nanodrugs. Therefore, the TEM micrographs support a conclusion that Zn(II) coordination generates more crystalline, uniform structures with potential for higher performance in biomedical applications

The peak for the aromatic ring proton showed a slight shift from 8.05 ppm in the ligand MTZ spectrum (Fig 5) to 8.06 ppm in both Mn and Zn complexes. This minimal change indicates that metal coordination barely affects the electronic environment of the aromatic ring protons because the aromatic ring was not directly involved in coordination. The OH proton shifts minimally from 5.04 ppm in MTZ to 5.03 ppm in both metal complexes, despite direct Mn bonding to the OH group. This small shift suggests a delicate balance of electron density withdrawal by the metal and possible changes in hydrogen bonding or molecular conformation, resulting in little net change in the chemical environment of the OH proton (Butera *et al*., 2023). The smaller shift of the OH proton in the Mn complex spectrum can be

attributed to weak ligand field effects of Mn ion. Earlier studies says that metals such as Mn tends to induce smaller ligand field perturbations on proton environments compared to heavier metals, resulting in only minor changes in chemical shifts even upon direct coordination (Kálmán *et al*., 2021). The methyl protons adjacent to the imine nitrogen (H of $CH_3C=N$) show a negligible shift from 4.41 ppm in MTZ to 4.40 ppm in the complexes. Even though the metal binds directly to the nitrogen, the methyl protons are only indirectly affected due to distance and shielding/deshielding interplay, causing minimal positional shift in the NMR spectrum ((Butera *et al*., 2023). For the Proton of CH_2-OH**,** no change is observed; the signal remains at 3.72 ppm across the free ligand and complexes. This indicates the CH_2 group was not involved in complexation and remains stable upon complexation. The methyl group proton shows a tiny shift from 1.36 ppm in free MTZ to 1.35 ppm in the complexes, reflecting a minor perturbation in the local chemical environment. The overall spectral data support stable complex formation where the metal interacts primarily with heteroatoms (N, O) but exerts minimal perturbation on protons nearby, consistent with reported studies of metallodrugs like metronidazole complexes with Mn and Zn (Starek *et al*., 2021).

The downfield shifts of C=N and aromatic carbons (Fig 6) confirm that the metal ions bind to the N1 atom, altering the electronic environment of the imidazole ring. This de-shielding effect is a hallmark of N-donor metal coordination in azole complexes (Dalton, 2017). The peaks for the side-chain $–CH_2$ groups observed at 59.73 ppm and 48.21 ppm were observed to have made shifts to 70.17 and 44.64 ppm in the Mn complex was ascribed to strain on the bonds due to electron density caused by coordination through the hydroxyl oxygen. In the Zn nano complex, these peaks were observed not to have made any shift providing strong evidence that MTZ coordinates only via the imidazole nitrogen side chain. The very minor shifts for imidazole CH_3 suggest coordination via the nitrogen (N1) atom rather than the ring carbon.

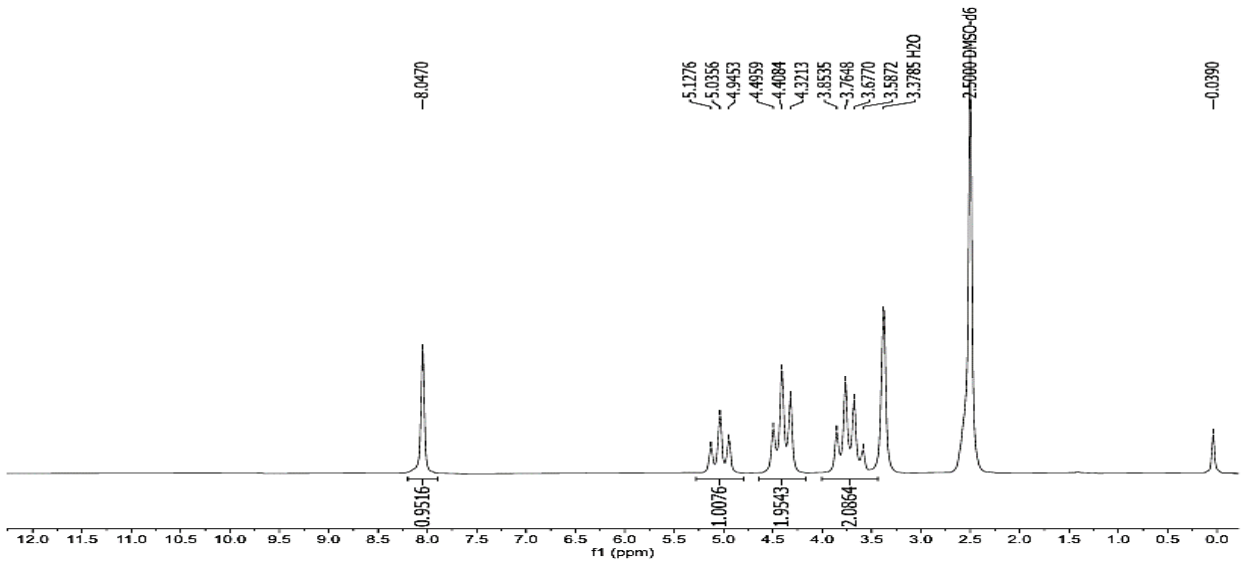

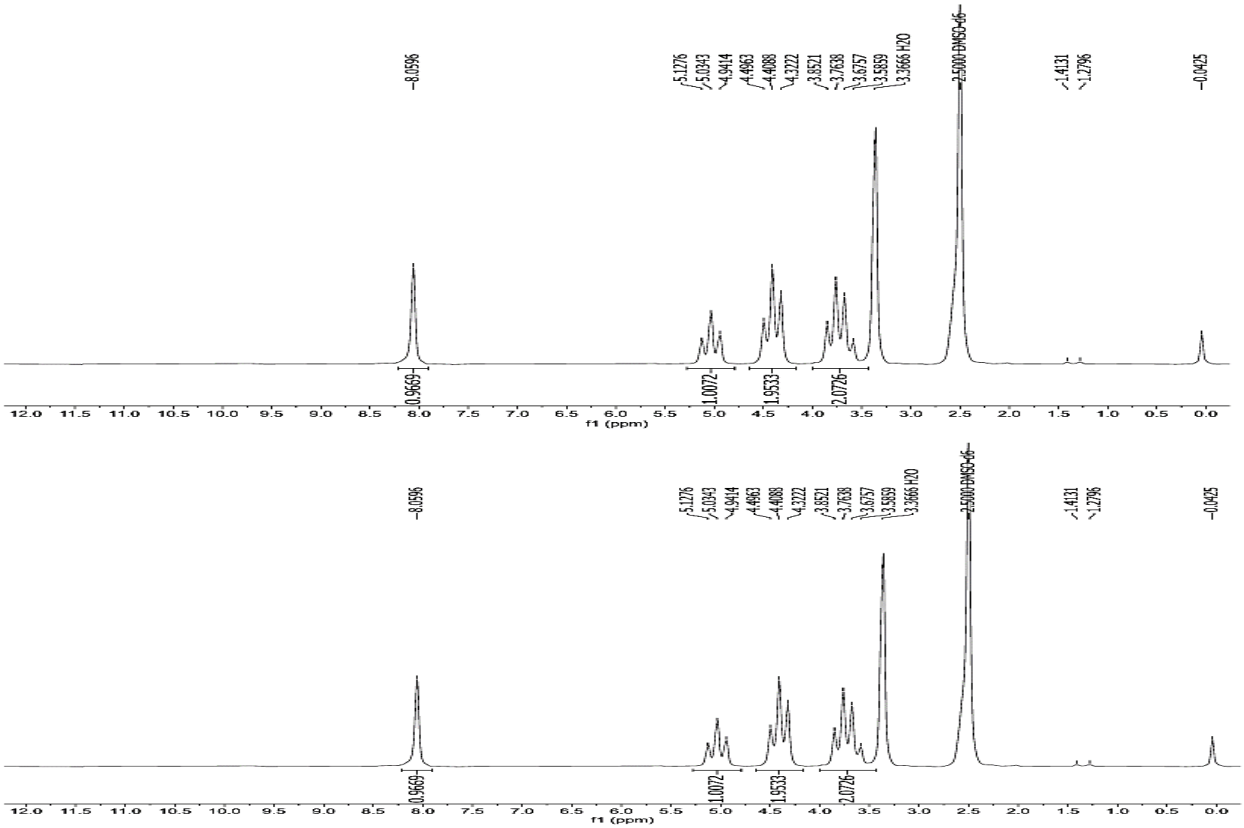

Fig 5: ^{1}H NMR spectra for MTZ, [Mn(MTZ)], [Zn(MTZ)]

The predictions (Table 3) revealed that the test compounds (nano-sized Mn (II) and Zn (II) complexes of metronidazole) has and retained favorable drug-likeness properties of the ligand MTZ. Some of which include the molecular weights of the complexes (397.25 and 407 g/mol) being within the acceptable range for oral drugs (< 500 g/mol) as given by Lipinski's rule of five (Lipinski *et al*., 2001). The number of hydrogen bond acceptors and hydrogen bond donors also remained at 8 and 2 respectively also falling within the acceptable range of 10 and 5 respectively (Veber *et al.,* 2002). This indicates that the coordination with metal ions did not adversely affect the critical interaction capabilities (Karuppiah *et al.,* 2025). The increase of the Topological Polar Surface Area (TPSA) value (which is necessary in predicting the cell membrane permeability) from 83.25 Å² in MTZ to 134.72 Å² in the metal complexes (still within the Lipinski's limit of 140 Å² suggests passive absorption characteristics (Ertl *et al*., 2000).

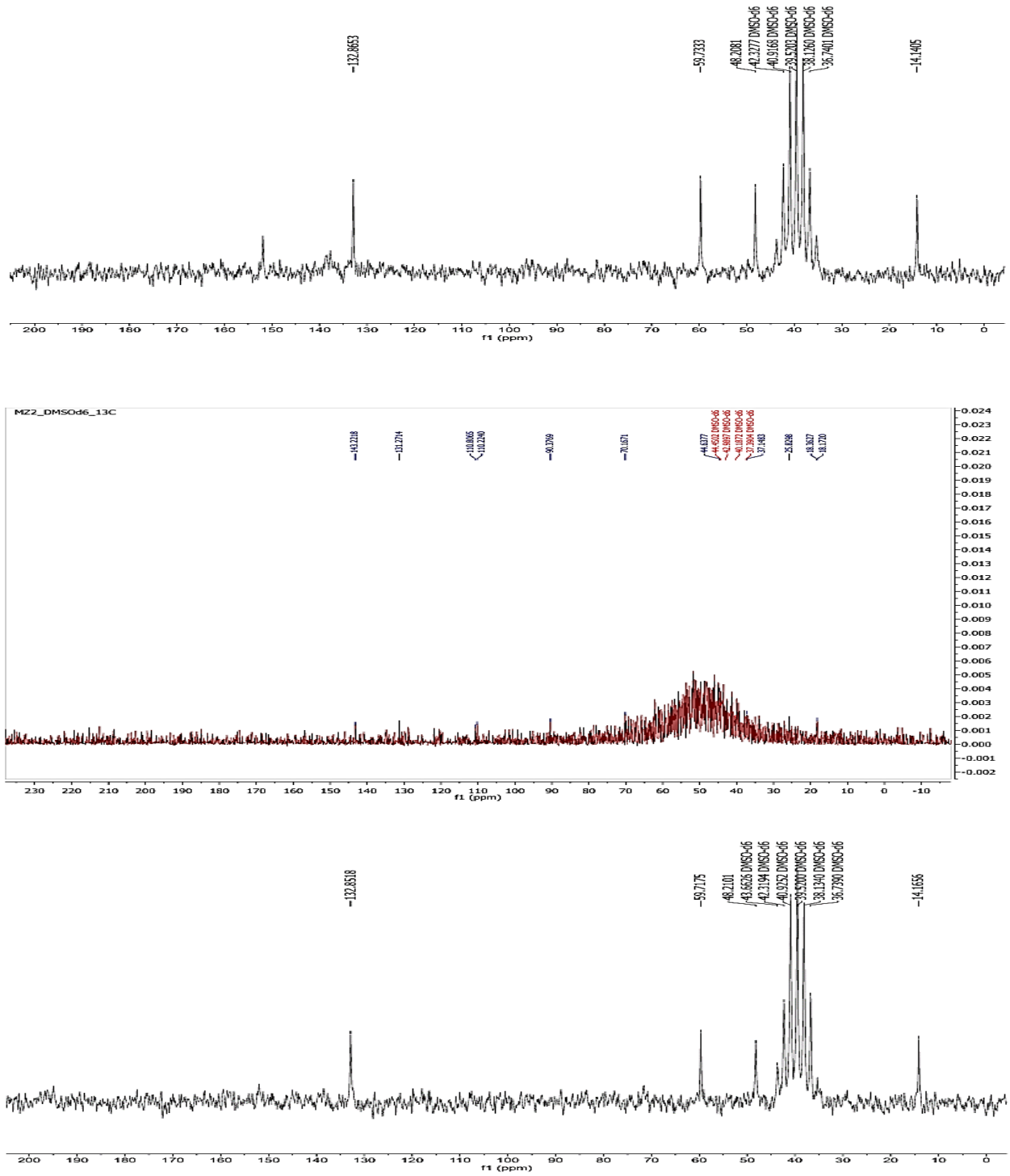

Fig 6: ^{13}C NMR spectra for MTZ, [Mn(MTZ)], [Zn(MTZ)]

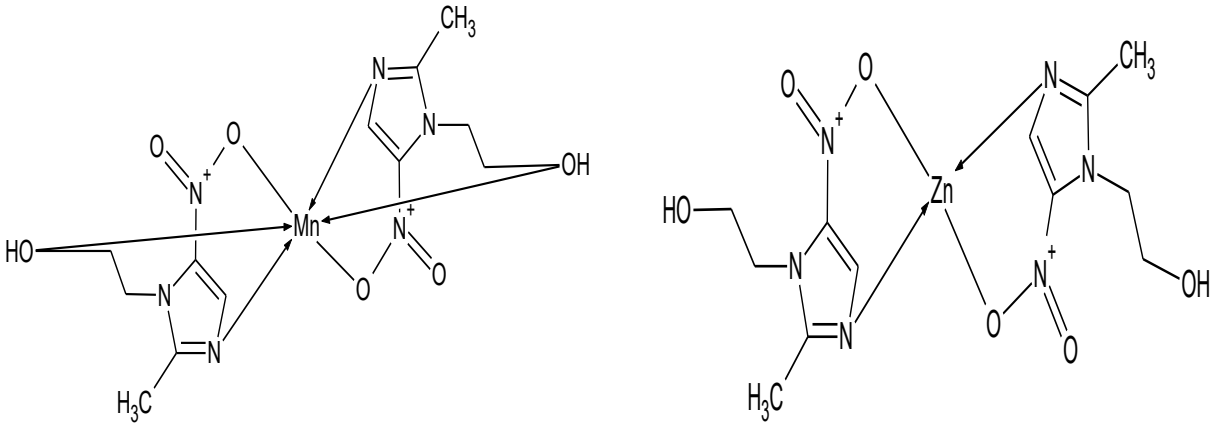

Fig 7: Proposed structure for [Mn(MTZ)] and [Zn(MTZ)]

In-silico evaluation of the synthesized Mn(II) and Zn(II) nanocomplexes was conducted to predict their physicochemical, drug-likeness, and ADME properties, which are critical parameters for early-stage drug design. Computational screening using SwissADME provides insight into molecular weight, hydrogen bonding capacity, lipophilicity, solubility, and oral bioavailability, while also assessing their compliance with drug-likeness rules such as Lipinski's criteria. These parameters collectively influence membrane permeability, absorption, metabolic behaviour and formulation feasibility. The predicted properties of metronidazole and its metal complexes are summarized in Table 3.

As shown in Table 3, the molecular weights of the Mn(II) and Zn(II) complexes increased to 397.25 g/mol and 407 g/mol, respectively, relative to the free ligand (171.15 g/mol), reflecting successful metal coordination. The number of hydrogen bond acceptors and donors increased from 4 and 1 in MTZ to 8 and 2 in both complexes, suggesting an enhanced potential for polar interactions, which is consistent with metal–ligand binding. An increase in molar refractivity from 43.25 in MTZ to 77.59 in the complexes further indicates an expanded electronic polarizability. The water solubility (Log S, ESOL) showed a slight reduction from −1.00 for MTZ to −1.52 and −1.59 for the Mn(II) and Zn(II) complexes; however, all the compounds remained classified as very soluble, supporting favourable dissolution behaviour. A considerable increase in TPSA from 83.25 Å² in MTZ to 134.72 Å² in the complexes suggests improved capacity for polar interactions but may also influence membrane diffusion pathways. The lipophilicity (log P) values shifted from −0.23 to −1.26 and −1.25 for the Mn and Zn complexes, indicating enhanced hydrophilicity.

All compounds displayed a bioavailability score of 0.55, indicating good oral absorption potential. The metal complexes showed a single Lipinski violation (N or O > 10), while the parent ligand had no violations, confirming that the complexes remain within acceptable drug-likeness limits for small molecules. None of the compounds triggered PAINS alerts, suggesting a low likelihood of assay interference. Synthetic accessibility values increased from 2.30 for MTZ to 3.33 and 3.20 for the Mn and Zn complexes, reflecting moderate additional effort required for synthesis due to metal coordination.

The water solubility (Log *S*) and class predict the nano metal complexes to be more soluble, the bioavailability score (0.55) predicts that the novel compounds would have a moderate oral absorption.

An improvement was observed in the lipophilicity (log *P*) prediction as the calculated log P values for the complexes are higher negative values suggesting an enhanced hydrophilic potential. This aligns with experimental observations of complex solubility in polar solvents like water (Daina *et al.,* 2017). One violation of the "number of rotatable bonds (NorO) > 10" rule was predicted for both complexes. This is a common occurrence for metallodrugs especially when the rigid coordination sphere increases the rotatable bond counts without necessarily impairing oral bioavailability (Zhang & Wilkinson, 2007). The high synthetic accessibility scores (3.20-3.33) and zero alerts in the PAINs (Pan-Assay Interference Compounds) assay indicate that these complexes are readily synthesized and not likely to exhibit false-positive results in biological screenings (Baell & Holloway, 2010).

Table 3: ADME, Physicochemical and Drug-Likeness Predictions

Compounds	MTZ	[Mn(MTZ)]	[Zn(MTZ)]
Molecular Weight in g/mol	171.15	397.25	407
No of Hydrogen bond acceptors	4	8	8
No of Hydrogen bond donors	1	2	2
Molar refractivity	43.25	77.59	77.59
Water solubility – Log *S* (ESOL)	-1.00	-1.52	-1.59
Water Solubility Class	Very soluble	Very soluble	Very soluble
TPSA value (Å²)	83.25	134.72	134.72
Lipophilicity (log *P*)	-0.23	-1.26	-1.25
No of Violations (Lipinski)	Yes; 0 violation	Yes;1 NorO>10	Yes; 1 NorO>10
Bioavailability score	0.55	0.55	0.55
PAIN assay (Med. Chem.)	0	0	0
Synthetic accessibility	2.30	3.33	3.20

To further assess the therapeutic potential of the synthesized nanometal complexes, pharmacokinetic properties were predicted using in-silico models. Key parameters such as gastrointestinal absorption, blood–brain barrier permeation, interaction with efflux transporters, and cytochrome P450 inhibition were evaluated to understand the absorption, distribution, and metabolic behaviour of the compounds. These computational profiles provide early screening insights for drug development, guiding decisions on compound selection for in-vitro and in-vivo evaluation. The pharmacokinetic predictions obtained for metronidazole and its Mn(II) and Zn(II) nanocomplexes are presented in **Table 4**.

As shown in **Table 4**, all compounds demonstrated high gastrointestinal absorption, suggesting that metal coordination does not compromise the oral uptake potential of metronidazole. None of the compounds were predicted to cross the blood–brain barrier, which is consistent with their high polarity and relatively low lipophilicity, and may reduce the risk of central nervous system-related side effects. The Mn(II) and Zn(II) complexes were predicted to be substrates of P-glycoprotein (P-gp), whereas MTZ was not, indicating a potential for efflux-mediated transport in intestinal and hepatic tissues.

Regarding metabolic interactions, both metal complexes showed a predicted inhibitory effect

on the CYP2C19 enzyme, while MTZ did not inhibit any of the evaluated cytochrome P450 isoforms. No inhibition was predicted for CYP1A2, CYP2C9, CYP2D6 or CYP3A4 for any of the compounds, suggesting a low risk of broad metabolic interference and drug–drug interactions through major P450 pathways. The predicted skin permeation (Log Kp) values decreased from −7.36 cm/s for MTZ to −9.19 and −9.26 cm/s for the Mn(II) and Zn(II) complexes, indicating reduced transdermal diffusion due to increased molecular size and polarity.

Generally, the pharmacokinetic data support favourable oral administration potential and a low likelihood of systemic metabolic complications, highlighting the suitability of the Mn(II) and Zn(II) nanocomplexes for further drug development studies.

Table 4: Pharmacokinetic predictions

Compounds	MTZ	[Mn(MTZ)]	[Zn(MTZ)]
Gastro-Intestinal absorption	High	High	High
Blood Brain Barrier permeant	No	No	No
P-gp substrate	No	Yes	Yes
CYP1A2 inhibitor	No	No	No
CYP2C19 inhibitor	No	Yes	Yes
CYP2C9 inhibitor	No	No	No
CYP2D6 inhibitor	No	No	No
CYP3A4 inhibitor	No	No	No
Log K_p (Skin permeation)(cm/s)	-7.36	-9.19	-9.26

The pharmacokinetic predictions (Table 4) gave that both [Mn(MTZ)] and [Zn(MTZ)] shared some key characteristics with the ligand MTZ. A high gastrointestinal (GI) absorption, which is essential property for oral drug administration (Veber *et al*., 2002) was predicted for all compounds. Also, like the ligand MTZ, the complexes are predicted to be non-permeants of the blood-brain barrier (BBB), which possibly reduces the potential neurotoxic side effects of the compounds. However, the nano complexes are predicted to be substrates for P-glycoprotein (P-gp). P-glycoprotein is an efflux transporter having the capacity of limiting their intracellular accumulation and potentially contribute to resistance (Wang *et al*., 2016).

In the metabolism prediction, the nano complexes are predicted to be inhibitors of the CYP2C19 isoenzyme, but not of other major cytochromes like CYP1A2, CYP2C9, CYP2D6, or CYP3A4. This suggests a relatively low risk of extensive metabolism by the cytochrome P450 enzymes and a very much reduced potential for drug-drug interactions via these specific pathways (Rendic & Guengerich, 2015). The skin permeation predictions gave coefficients (Log Kp < -9 cm/s) are very low, indicating poor transdermal absorption. This aligns with typical administration route of MTZ being oral or intravenous and so limits their possible use in tropical applications.

Ttoxicity profile prediction (Table 5) indicates that the metal complexes just like the ligand exhibit favorable safety profile. Both the ligand and the metal complexes ([Mn(MTZ)] and [Zn(MTZ)]) are classified under Toxicity Class IV, which is defined by a predicted LD_{50} range of 500-5000 mg/kg. This toxicity class shows that the compounds have low acute oral toxicity (Drwal *et al*., 2014). A prediction accuracy of 67.38% was predicted for both complexes and the average similarity to known toxic compounds (59.14% for Mn and 56.81%

for Zn). These predicted values provide a reasonable level of confidence in these predicted results which suggest that metal complexation did not introduce significant acute toxicity risks to the metronidazole compound.

Table 5: Toxicity predictions

Compounds	MTZ	[Mn(MTZ)]	[Zn(MTZ)]
Predicted LD_{50} in mg/kg	1500	1500	1500
Predicted Toxicity Class	IV	IV	IV
Average similarity in %	73.51	59.14	56.81
Prediction Accuracy %	69.26	67.38	67.38

4.0 Conclusion

This study successfully synthesized Mn(II) and Zn(II) nanometal complexes of metronidazole using a sonochemical approach, producing stable crystalline nanocomplexes with high yields of 82% and 78%, respectively. Initial physical assessments, including colour change and increased melting points from 160 °C in the free ligand to 207 °C and 203 °C in the Mn and Zn complexes, confirmed effective metallation. The solubility profiles showed that both complexes remained soluble in polar solvents and water, demonstrating that metal coordination did not compromise the hydrophilicity of metronidazole.

Spectroscopic and structural analyses provided consistent evidence of complex formation. UV–visible spectra showed characteristic $\pi\rightarrow\pi^*$ and $n\rightarrow\pi^*$ transitions, while FTIR shifts of the C=N and NO_2 bands confirmed binding through the imidazole nitrogen and nitro oxygen. XRD revealed distinct crystalline phases for Mn and Zn complexes with nanoscale crystallite sizes of 61.6 nm and 48.1 nm, respectively, indicating metal-dependent nucleation behaviour. TEM images showed particle sizes in the 2.22–10.80 nm range, confirming the nanoscale character of the products, with Zn complexes exhibiting greater particle uniformity. NMR analyses showed minimal perturbation of proton environments, supporting coordination through heteroatoms, primarily N1, consistent with the proposed structures.

In-silico predictions confirmed that both metal nanocomplexes retain favourable drug-likeness parameters within Lipinski's limits, with molecular weights below 500 g/mol, acceptable hydrogen-bonding properties, and good bioavailability scores (0.55). An increase in TPSA values to 134.72 $Å^2$ suggests enhanced polarity and potential for passive absorption. Pharmacokinetic predictions indicate high gastrointestinal absorption for both complexes and no blood–brain barrier permeability, while identifying predicted interactions with CYP2C19 and P-glycoprotein transport pathways.

Overall, the combined experimental and computational results demonstrate the successful formation of Mn(II) and Zn(II) nanometronidazole complexes with improved physicochemical properties, nanoscale structural features and promising oral absorption characteristics. These findings suggest the potential applicability of the nanocomplexes as enhanced antimicrobial agents, providing a strong basis for further biological evaluation and formulation studies.

5.0 References

Lofmark, S., Edlund, C., & Nord, C. E. (2010). Metronidazole is still the drug of choice for treatment of anaerobic infections. *Clinical Infectious Diseases*, 50(Supplement_1), S16-S23.

Singh, N., K., Singh, S., B., & Muthu, S. (2012). Synthesis, characterization, and biological activities of some metal

complexes of metronidazole. *Journal of Coordination Chemistry*, 65(8), 1319-1330.

Otuokere, I. E., Ohwimu, J. G., Amadi, K. C., Alisa, C. O., Nwadire, F. C., Igwe, O. U., Okeyeagu, A. A. & Ngwu, C. M. (2019). Synthesis, Characterization and molecular Docking studies of Mn (II) complex of sulfathiazole. *Journl of the Nigerian Society of Physical Sciences,* 1(3), 95-102.

Asogwa, B. C. & Otuokere, I. E. (2024) Sonochemical synthesis and characterization of Fe (II) and Cu (II) nano-sized complexes of sulfamethoxazole. *Journal of the Nigerian Society of Physical Sciences* 6 (2024) 2011.

Otuokere, I. E., Onyenze, U. & Igwe, J. C. (2016). Co (II) and Fe (II) mixed ligand complexes of Perfloxacin and Ascorbic Acid: Synthesis, Characterization and Antibacterial Studies. *Research Journal of Science and Technology,* 8, 4, 215-220.

Guo, Z., & Sadler, P. J. (2000). *Metals in medicine*. Angewandte Chemie International Edition, 39, 9, 1512–1531.

Otuokere, I. E, Okorie, D. O. Asogwa, B. C., Amadi, K. O., Ubani, L. O. C. & Nwadire, F. C. (2017) Spectroscopic and Coordination Behavior of Ascorbic Acid Towards Copper (II) Ion. *Research in Analytical and Bioanalytical Chemistry,* 1, 1, 1-7.

Robert, O. F., Otuokere, I. E. & Nnaji, J. C. (2025). Synthesis, Characterization, and ADME/T Prediction of (2Z)-2-[2-(2,4-Dinitrophenyl)hydrazinylidene]-1,2-diphenyle -than-1-ol (DPHD) and Its Copper (II) Complex. *Communication in Physical Sciences,* 12, 7, 2060-2075.

Andreini, C., Bertini, I., Cavallaro, G., Holliday, G. L., & Thornton, J. M. (2008). Metal ions in biological catalysis: from enzyme databases to general principles. JBIC Journal of Biological Inorganic Chemistry, 13(8), 1205–1218.

Asogwa, B. C., Mac-kalunta, O.M., Iheanyichukwu, J. I., Otuokere, I. E. and Nnochirionye, K. (2024) Sonochemical synthesis, characterization and ADMET studies of Fe (II) and Cu (II) nano-sized complexes of trimethoprim. *Journal of the Nigerian Society of Physical Sciences* 6 (2024) 2048.

Smith, V. J., Witika, B. A. & Walker, R. B. (2020). Quality by Design Optimization of Cold Sonochemical Sythesis of Zidovudine-Lamivudine Nanosuspensions. *Pharmaceutics,* 12, 4, 367.

Lee, S., Xu, H., Xu, H. & Neuefeind, J. (2021). Crystal Structure of Moganite and its Anisotropic Atomic Displacement Parameters Determined by Synchrotron X-ray Diffraction and X-ray/Neutron Pair Distribution Function Analyses. *Minerals,* 11, 3, 272.

Asogwa, B. C. and Otuokere, I. E. (2024) *In-silico* Studies of Fe (II) And Cu (II) Metal Complexes of Sulfamethoxazole. A research paper presented during the AbiaChem maiden conference MOUAU 23rd – 25th July 2024.

Otuokere, I.E., Iheanyichukwu, J.I., Asogwa, B.C., Mac-kalunta, O.M. *et al.* (2025). GC–MS, antioxidant, anti-infammatory and in silico studies of the polyherbal formulation containing *Mangifera indica*, *Psidium guajava*, *Cymbopogun citratus* and *Azadirachta indica. Discover Chemistry* 2, 121.

Otuokere, I.E., Iheanyichukwu, J.I., Asogwa, B.C., Mac-kalunta, O.M. *et al.* (2025) Network pharmacology and molecular docking to reveal the pharmacological mechanisms of *Abelmoschus esculentus* (l.) moench in treating breast cancer. *In Silico Pharmacology* **13**, 40.

Daina, A., Michielin, O., & Zoete, V. (2017). SwissADME: a free web tool to evaluate pharmacokinetics, drug-likeness and

medicinal chemistry friendliness of small molecules. Scientific Reports, 7, 42717.

Trupti, P., Suresh, G., Khanderao, P., Shreyas, P. and Rajeshwari, O. (2019). A Review on Bio-Synthesized Co_3O_4 Nanoparticles using Plant Extracts and Their Diverse Applications, *Journal of Chemical Reviews*, 1(4): 260-270.

Ndahi , N. P., Yahaya, N. P., Bako, L., Madugu, M. L., & Zulqiflu, A. (2018). Synthesis and Partial Characterization of Two Schiff Base Ligands with (2 and 4-Nitroaniline) and their Transition Metal (II) (Co and Cu) Complexes. *Nigerian Journal of Pharmaceutical and Biological Research,* 3, 1, 53-59.

Edozie, O. I., Godday, O. J., Chijioke, A. K., Uchenna, I. O., & Chigozie, N. F. (2020). Synthesis, characterization and molecular docking studies of Co (II) metal complex of sulfathiazole. *Bulletin of the Chemical Society of Ethiopia,* 34, 1, 83 – 92.

Onyegbule, F.A., and Uche, C.I. (2021). UV-Vis spectroscopic studies of metronidazole-metal complexes. *Journal of Molecular Structure. 1225*, 129133.

Sadeek, S.A., and El-Shwiniy, W.H. (2015). Metal complexes of metronidazole: Spectroscopic and thermal studies. *Spectrochimica Acta Part A,* 136: 1673-1679.

El-Wahab H. A., Atta, M., Hassan, W. A., & Nasser, A. M. (2019). Preparation, characterization and evaluation of some acrylate polymers nanoparticles as binder to improving the physicl properties of water based paints. *International Journal of Nanoparticles Nanotechnology,* 5, 022.

Sadeghi, S., & Azhdari, A. (2013). A theoretical study of blue-shifting hydrogen bonds in π weekly bound complexes. *Spectrochimica ACTA Part A: Molecular and Biomolecular Spectroscopy,* 104, 141-147.

Jones, P.R., and Zhang, Y. (2019). Crystallinity in Mn (II) coordination polymers. *Crystal Engineering Communications.* 21(12), 1892-1901.

Brown, M.E., Smith, T.R., and Jones, P.R. (2018). Nucleation kinetics of transition metal complexes. *Crystal Growth and Design. 18*(5): 2743-2751.

Taylor, M.J., and Li, Y. (2022). Zinc-drug complexes: Structural diversity and applications. *Coordination Chemistry Reviews.* 451, 214274.

Smith, T.R., and Brown, M.E. (2019). Influence of manganese on drug efficacy. *Journal of Coordination Chemistry,* 72(5), 1029-1037.

Butera, V., D'Anna, L., Rubino, S., Bonsignore, R., Spinello, A., Terenzi, A., & Barone, G. (2023). How the metal ion affects the 1H NMR chemical shift values of Schiff base metal complexes: Rationalization by DFT calculations. *The Journal of Physical Chemistry A, 127*(44): 9283–9290.

Kálmán, F. K., Nagy, V., Uzal-Varela, R., Pérez-Lourido, P., Esteban-Gómez, D., Garda, Z., Pota, K., Mezei, R., Pallier, A., Tóth, É., Platas-Iglesias, C., & Tircsó, G. (2021). Expanding the ligand classes used for Mn (II) complexation: Oxa-aza macrocycles make the difference. *Molecules, 26*(6): 1524 -1530.

Starek, M., Dąbrowska, M., Chebda, J., Żyro, D., & Ochocki, J. (2021). Stability of metronidazole and its complexes with silver(I) salts under various stress conditions. *Molecules, 26*(12): 3582 - 3590

Dalton Trans. (2016). Special issue: Metal-drug complexes in medicine. *Dalton Transactions, 45*(45): 17817-18024.

Lipinski, C. A., Lombardo, F., Dominy, B. W., & Feeney, P. J. (2001). Experimental and computational approaches to estimate solubility and permeability in drug discovery and development settings. Advanced Drug Delivery Reviews, 46(1-3), 3–26.

Veber, D. F., Johnson, S. R., Cheng, H. Y., Smith, B. R., Ward, K. W., & Kopple, K. D. (2002). Molecular properties that influence the oral bioavailability of drug candidates. Journal of Medicinal Chemistry, 45(12), 2615–2623.

Karuppiah, N., Karthikeyan, A., Otuokere, I. E., Velmurugan, G., Muthukkumar, M., Sandhanasamy, D., Subramanian, R., Raja, K., Rameshkumar, S. (2025). Synthesis, Crystal Structure and Computational Investigation of Zinc-Cytosine Coordination Complex: Insights From Molecular Docking, ADME Prediction, HOMO-LUMO and MEP Analysis. *Applied Organometallic Chemistry,* 39, 6

Ertl, P., Rohde, B., & Selzer, P. (2000). Fast calculation of molecular polar surface area as a sum of fragment-based contributions and its application to the prediction of drug transport properties. Journal of Medicinal Chemistry, 43(20), 3714–3717.

Zhang, M. Q., & Wilkinson, B. (2007). Drug discovery beyond the 'rule-of-five'. Current Opinion in Biotechnology, 18(6), 478–488.

Baell, J. B., & Holloway, G. A. (2010). New substructure filters for removal of pan assay interference compounds (PAINS) from screening libraries and for their exclusion in bioassays. Journal of Medicinal Chemistry, 53(7), 2719–2740.

Wang, L., Wang, C., & Liu, Q. (2016). The role of P-glycoprotein in drug resistance in cancer chemotherapy. Oncology Letters, 11(2), 817-822.

Rendic, S., & Guengerich, F. P. (2015). Survey of human oxidoreductases and cytochrome P450 enzymes involved in the metabolism of chemicals. Chemical Research in Toxicology, 28(1), 38–42.

Drwal, M. N., Banerjee, P., Dunkel, M., Wettig, R. M. & Preissner, R. (2014). Protox: a web server for the *in silico* prediction of rodent oral toxicity. *Nucleic Acids Research,* 42, W1, W53-W58.

Declaration

Funding sources

No funding

Competing Statement

There are no competing financial interests in this research work.

Ethical considerations

Not applicable

Data availability

The microcontroller source code and any other information can be obtained from the corresponding author via email.

Authors' Contribution

George I. Etim carried out the experimental work. Brendan C. Asogwa interpreted the results, drafted the initial manuscript. Ifeanyi E. Otuokere conceptualized and supervised the study, led in result interpretation and contributed to manuscript revision. Kelvin O. Amadi supervised the research and critically reviewed the manuscript.